Molecular Dynamics Simulation of the α-D-Man*p*-(1 → 3)-β-D-Glc*p*-OMe Disaccharide in Water and Water/DMSO Solution

Aleksey Vishnyakov,[†] Göran Widmalm,[‡] Jozef Kowalewski,[§] and Aatto Laaksonen*[,§]

Contribution from the Department of Organic Chemistry and Division of Physical Chemistry, Arrhenius Laboratory, Stockholm University, S-106 91 Stockholm, Sweden

Received October 5, 1998. Revised Manuscript Received March 9, 1999

Abstract: Molecular dynamics simulation studies of solvation structure, conformational behavior, and dynamics of α-D-Man*p*-(1 → 3)-β-D-Glc*p*-OMe in water and in the binary 1:3 molar mixture of dimethylsulfoxide and water are reported. Several combinations of different force fields are evaluated for both the disaccharide and the solvent components. The disaccharide molecule is found to be fairly rigid, showing no high-amplitude rotation around the glycosidic linkage, which is consistent with previous experimental findings. Also, the preferred conformation of the disaccharide in the water simulation is in agreement with experiment. The predominant conformation of α-D-Man*p*-(1 → 3)-β-D-Glc*p*-OMe in the water−dimethylsulfoxide solution was found to be dependent on the potential models for the solvent components, thus stressing the importance to carefully evaluate the potentials used against available experimental data. In general, the different hydroxyl groups of the disaccharide prefer different solvent components as hydrogen bond acceptors.

I. Introduction

Carbohydrates are found on cell surfaces as glycolipids or glycoproteins.[1] They are involved in cell−cell recognition, usually via carbohydrate−protein interactions. During the last decade, carbohydrate−carbohydrate interactions have also been shown to be of importance.[2] For a detailed description of the full three-dimensional structure of a carbohydrate molecule, a number of aspects should be addressed, namely, its conformation, flexibility, dynamics, hydrophilic vs hydrophobic properties, as well as its electrostatics. A powerful approach to studies of these molecules is to combine information from computer simulations with experimental data. This is particularly important in order to validate the use of simulations when addressing problems for which only limited experimental data are available.[3]

NMR spectroscopy is a very important technique for examining carbohydrates and their properties.[4] It provides various types of data which can be used for examination of the structure and dynamics of biomolecules. These include homo- and heteronuclear Overhauser effects (NOEs), homo- and heteronuclear long-range spin−spin coupling constants, and spin−lattice and spin−spin relaxation rates. Some of these were recently applied for description of the dynamical behavior of the disaccharide α-D-Man*p*-(1 → 3)-β-D-Glc*p*-OMe.[5] It was found that intra-ring proton cross-relaxation could be explained using the motional parameters obtained from the carbon-13 NMR data. Furthermore, *trans*-glycosidic proton cross-relaxation displayed the same field dependence as intra-residue cross-relaxation. NMR data were also used to calculate distances between protons in the molecule, without using a molecular model and a reference distance, which is the usual way to deal with biomolecules of this type. An intra-residue distance in the mannosyl group was found to be in good agreement with that obtained from an energy-minimized molecular mechanics model. Also in accordance with the result of molecular modeling, the *trans*-glycosidic distance from the anomeric proton on the mannosyl group to the proton at the linkage position was found to be shorter than the intra-residue distance. However, the molecular modeling in the previous study[5] was restricted to potential energy minimization. Additional molecular dynamics simulation on this system would be of interest, in particular since a comparison to experimental data can be made.

Molecular dynamics (MD) simulations of carbohydrates in aqueous solutions started about a decade ago. One of the early simulations was that of glucose in water.[6] An omnipresent question for carbohydrates is the influence of solvent, usually water,[7] on the population distributions of different conformational states and dynamics of conformational transitions of the solute. Another important problem concerning the carbohydrates is the solvent structure around a solute. This is usually described in terms of radial pair distribution functions between different solute and solvent sites. In the case of aqueous solutions of carbohydrates, these are primarily oxygens and hydroxyl protons of saccharide and water. More recently, the analysis of hydration has focused on the anisotropic solvent structuring.[8] Several investigations have been performed that give an insight into the ordering of water molecules around carbohydrates (see, e.g., refs 9 and 10).

[†] Department of Chemistry, St. Petersburg State University.
[‡] Department of Organic Chemistry, Arrhenius Laboratory, Stockholm University.
[§] Division of Physical Chemistry, Arrhenius Laboratory, Stockholm University.

(1) Dwek, R. A. *Chem. Rev.* **1996**, *96*, 683−720.
(2) Pavelka, M. *Glycosciences*; Gabius, H.-J., Gabius, S., Eds.; Chapman & Hall: London, 1997, pp 277−289.
(3) van Gunsteren, W. F.; Mark, A. E. *J. Chem. Phys.* **1998**, *108*, 6109−6116.
(4) Landersjö, C.; Stenutz, R.; Widmalm, G. *J. Am. Chem. Soc.* **1997**, *119*, 8695−8698.
(5) Mäler, L.; Widmalm, G.; Kowalewski, J. *J. Phys. Chem.* **1996**, *100*, 17103−17110.
(6) Brady, J. W. *J. Am. Chem. Soc.* **1989**, *111*, 5155−5164.
(7) Engelsen, S. B.; Perez, S. *Carbohydr. Res.* **1996**, 21−38.
(8) Liu, Q.; Brady, J. W. *J. Am. Chem. Soc.* **1996**, *118*, 12276−12286.

10.1021/ja9835180 CCC: $18.00
Published on Web 05/27/1999

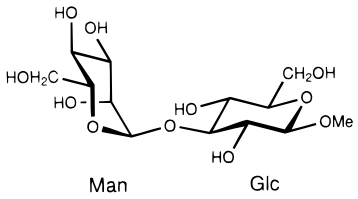

Figure 1. Schematic drawing of α-D-Man*p*-(1 → 3)-*β*-D-Glc*p*-OMe.

Several different force fields have been developed specifically for molecular simulations of carbohydrates. None of them, however, has yet gained a widespread acceptance in the scientific community as the force field of choice. Although the available force fields usually give similar preferences for carbohydrate conformations, and even for hydration structure, several details can be quite different, and the agreement with experiment is not always convincing. The most obvious explanation for discrepancies between simulated and experimental results is insufficient parametrization of the force field, in particular, the glycosidic regions. Of course, when different force fields give a similar picture of the molecule but the agreement with the experiment is poor, the discrepancy can be sought in the way in which the comparison to experimental data is performed. To illustrate this, we can choose the *trans*-glycosidic heteronuclear ^3J(C,H) coupling constant as an example. This is a typical experimentally accessible parameter. In recent studies, using force fields such as HSEA, CHEAT95, or PARM22, agreement[11] as well as disagreement[12] with experiments were observed, when the ^3J(C,H) values were calculated over the trajectories based on one Karplus type of relationship. However, it was evident from the latter study that since the atoms substituting the coupling pathway are different, carbon/oxygen vs. carbon/carbon, for the ϕ and ψ torsional angles, respectively, a more specific Karplus relationship for each of them should be appropriate.

In the present work we have extended the previous experimental studies on the disaccharide α-D-Man*p*-(1 → 3)-*β*-Glc*p*-OMe by carrying out molecular dynamics simulations in solution, using both water and a mixture of water and dimethylsulfoxide (DMSO) as solvents. Analyses of the conformational structure and dynamics have been performed together with an investigation of the solvent structuring. The latter is done based on both radial distribution functions (RDF) and spatial distribution functions (SDF) in three dimensions.[13] In addition, analysis of the hydrogen bonds and their lifetimes is carried out. Comparison with high quality data from NMR experiments is given and some aspects of the dynamical behavior of α-D-Man*p*-(1→ 3)-*β*-D-Glc*p*-OMe are included. Regular hexopyranoses, i.e., sugars like glucose and mannose in the ring-form shown in Figure 1, are α- or *β*-linked via O1 and can be substituted at O2, O3, O4, and O6. The disaccharide subject to the present study serves as a model substance and resembles two disaccharide elements found in nature in polysaccharides and glycoproteins, viz., α-D-Glc*p*-(1 → 3)-α-D-Glc*p* and α-D-Man*p*-(1 → 3)-α-D-Man*p*, respectively.

It should be mentioned that the mixed solvent, viz., water to DMSO in a molar ratio of 7 to 3[5] facilitates low-temperature studies. In the experimental work, this more viscous cryosolvent was used in order to increase the global correlation time of the solute. For relatively small oligosaccharides, this puts the molecular motion outside the extreme narrowing region, i.e., when $\omega\tau_c \ll 1$, thus making magnetic field dependent studies possible. In general, no large changes in conformation upon alteration of the solvent, i.e., between water and the mixture, have been found using experimental NMR data, e.g., ^{1}H,^{1}H NOEs, and *trans*-glycosidic ^3J(C,H) values (see refs 12 and 14).

II. Models and Simulation Details

Two force fields have been used for the disaccharide: the GLYCAM_93 parameter set,[15] based on the AMBER force field, and the OPLS potential function for carbohydrates, recently proposed by Damm et al.[16] Both force fields introduce a new atomic type for the anomeric carbon. In addition, unique values of force constants for covalent bonds and angles are specified for α and *β* anomers in the GLYCAM force field, as well as a new atom type for the glycosidic oxygen. Torsional parameters were optimized, based on ab initio calculations carried out on substituted tetrahydropyrans. For the OPLS set, Damm et al.[16] derived torsional parameters by fitting them to results form restricted Hartree−Fock (RHF) calculations of hexoses.

Following the usual approach in the OPLS force field, the nonbonded parameters were assigned by dividing the structure of α-D-Man*p*-(1 → 3)-*β*-D-Glc*p*-OMe into several smaller alcohol- or ether-like fragments, each of which was made electro-neutral. Partial charges and Lennard-Jones parameters, optimized for liquid ethers and alcohols,[17,18] were assigned to each atom.

Partial charges for the use with the GLYCAM parameter set were calculated at the RHF/6-31G* level with the Gaussian 94 package.[19] Table 1 gives the partial charges for oxygens and hydroxyl protons. The values of the two sets of charges in Table 1 agree well with each other as well as with those for CHARMM but have substantially higher absolute values than the corresponding CNINDO/2RF and AM1 charges, used in other work.[20,21]

Because of the noticeable model dependence in the water structuring around carbohydrates in previous simulations,[22] we have evaluated two different water models as a solvent: the rigid TIP3P[23] and the flexible SPC[24] models. The choice of DMSO models is more limited.[25] The available models give good results for both the structure and diffusion in liquid DMSO. How the existing DMSO models behave in a water−DMSO mixture has not been investigated thoroughly yet. For the present

(9) Brady, J. W.; Schmidt, R. K. *J. Phys. Chem.* **1993**, *97*, 958−966.
(10) Liu, Q.; Schmidt, R. K.; Teo, B.; Karplus, P. A.; Brady, J. W. *J. Am. Chem. Soc.* **1997**, *119*, 7857−7862.
(11) Höög, C.; Widmalm, G. *Glycoconjugate J.* **1998**, *15*, 183−186.
(12) Rundlöf, T.; Kjellberg, A.; Nishida, T.; Damberg, C; Widmalm, G. *Magn. Reson. Chem.* **1998**, *36*, 839−847.
(13) Svishchev, I. M.; Kusalik, P. G. *J. Chem. Phys.* **1993**, *99*, 3049−3058.
(14) Widmalm, G.; Byrd, R. A.; Egan W. *Carbohydr. Res.* **1992**, *229*, 195−211.
(15) Woods, R. J.; Dwek, R. A.; Edge, C. J.; Fraser-Reid, B. *J. Phys. Chem.* **1995**, *99*, 3832−3846.
(16) Damm, W.; Frontera, A.; Tirado-Rives, J.; Jorgensen, W. L. *J. Comput. Chem.* **1997**, *18*, 1955−1970.
(17) Jorgensen, W. L.; Maxwell, D. S.; Tirado-Rives, J. *J. Am. Chem. Soc.* **1996**, *118*, 11225−11236.
(18) Jorgensen, W. L.; Damm, W.; Frontera, A.; Lamb, M. L.; *NATO ASI Ser., Ser. C* **1996**, *485*, 115.
(19) Frisch, M. J.; Trucks, G. W.; Schlegel, H. B.; Gill, P. M. W.; Jonson, B. G.; Robb. M. A.; Cheeseman, J. R.; Keith, T.; Petersson, G. A.; Raghavachari, K.; Al-Laham. M. A.; Zakrzewski, V. G.; Ortiz, J. V.; Foresman, J. B.; Cioslovski, J.; Stefanov, B. B.; Nanayakkara, A.; Challakombe, M.; Peng, C. Y.; Ayala, P. Y.; Chen, W.; Wong, M. W.; Anders, J. L.; Replodge, E. S.; Gomperts, R.; Martin, R. L.; Fox, D. J.; Binkley, J. S.; Defrees D. J.; Baker, J.; Stewart, J. P.; Heal-Gordon, C.; Gonzales, C.; Pople, J. A. Gaussian 94, Revision B. 2, Gaussian Inc., Pittsburg, PA, 1995.
(20) Edge, C.; Singh, U.; Bazzo, R.; Taylor, G. L.; Dwek, R. A.; Rademacher, T. W. *Biochemistry* **1994**, *90*, 2731−2735.
(21) Donnamaria, M. C.; Howard, E. I.; Grigera, J. R. *J. Chem. Soc., Faraday Trans.* **1994**, *90*, 2731−2735.
(22) Liu, Q.; Brady, J. W. *J. Phys. Chem. B* **1997**, *101*, 1317−1321.

Table 1. Atomic Partial Charges[a]

atom	RHF/6-31G*	OPLS	atom	RHF/6-31G*	OPLS
C1′	0.572	0.300	C1	0.299	0.300
H1′	0.048	0.100	H1	0.097	0.100
C2′	−0.037	0.205	C2	0.0904	0.205
H2′	0.155	0.060	H2	0.138	0.060
C3′	0.434	0.205	C3	0.047	0.170
H3′	0.074	0.060	H3	0.119	0.030
C4′	−0.079	0.205	C4	0.061	0.205
H4′	0.084	0.060	H4	0.127	0.060
C5′	0.305	0.170	C5	−0.130	0.170
H5′	0.034	0.030	H5	0.151	0.030
C6′	0.291	0.145	C6	0.316	0.145
H6A′	−0.008	0.060	H6A	−0.005	0.060
H6B′	0.068	0.060	H6B	0.068	0.060
O2′	−0.692	−0.700	O1	−0.467	−0.400
HO2′	0.431	0.435	O2	−0.656	−0.700
O3′	−0.769	−0.700	HO2	0.450	0.435
HO3′	0.475	0.435	O3	−0.416	−0.400
O4′	−0.721	−0.700	O4	−0.691	−0.700
HO4′	0.489	0.435	HO4	0.454	0.435
O5′	−0.584	−0.400	O5	−0.331	−0.400
O6′	−0.730	−0.683	O6	−0.713	−0.683
HO6′	0.444	0.418	HO6	0.459	0.418
			CMe	0.164	0.110
			H1Me	−0.004	0.030
			H2Me	0.062	0.030
			H3Me	0.024	0.030

[a] Obtained using RHF/6-31G* ab initio calculations and the OPLS strategy, used in the present simulation with GLYCAM 93 and OPLS parameter sets, respectively.

study we have chosen the P2 and OPLS[26,27] models for DMSO, to be used with the SPC and TIP3P water models, respectively. The heat of evaporation and the diffusion coefficient for liquid DMSO, obtained with these two models, are in good agreement with the experimental data.[25] The P2−SPC model for the water−DMSO binary system also reproduces the experimental radial distribution functions in the mixture[26] with reasonable accuracy.

In the initial part of the simulation, the disaccharide molecule was placed in a cavity, surrounded by 256 solvent molecules, arranged as a face-centered cubic lattice and a density of 0.6 g/cm^3. During the first 5 ps of trajectories the volume of the cubic simulation box was gradually compressed to a density of 1.020 g/cm^3. This was followed by a 40 ps NVT simulation keeping the solute molecule rigid, while a preliminary equilibrium in the solvent was established. Thereafter the simulation was carried out in the NPT ensemble at $P = 1.0$ atm. The MD simulations were carried out at $T = 288$ K, both in aqueous solution and in water−DMSO (3:1) solutions.

We recorded three 1.0 ns trajectories for the α-D-Man*p*-(1 → 3)-β-D-Glc*p*-OMe−water system using different models, referred to as GLYCAM−SPC (W1), GLYCAM−TIP3P (W2), and OPLS−TIP3P (W3), and two 1.0 ns trajectories for α-D-Man*p*-(1 → 3)-3-D-Glc*p*-OMe in the mixed solvent, GLYCAM−SPC−P2 (M1), and GLYCAM−TIP3P−OPLS (M2) (a summary of the simulations is given in Table 2). Statistics for the systems behavior were collected over the last 800 ps of each trajectory. DMSO and TIP3P water were kept rigid using the SHAKE[28] algorithm. The temperature and pressure were

Table 2. Specification of the Simulations

run	models used: sugar	water	DMSO	ρ_{av}, g/cm^3
vacuum				
V1	GLYCAM			
V2	OPLS			
aqueous solution				
W1	GLYCAM	SPC		1.026
W2	GLYCAM	TIP3P		1.022
W3	OPLS	TIP3P		1.022
mixed solvent				
M1	GLYCAM	SPC	P2	1.075
M2	GLYCAM	TIP3P	OPLS	1.052

maintained by the Nóse−Hoover thermostat.[29,30] In addition, two 1.0 ns vacuum simulations, with the GLYCAM and OPLS potential functions, were recorded for comparison, with the temperature kept fixed using velocity scaling. The multiple time step method by Tuckerman et al.[31] was used in the simulations. Fast fluctuating forces from stretching of covalent bonds and angles were calculated at 0.2 fs, while a time step of 1.0 fs was used for other interactions. All of the simulations were carried out on a dual 300 MHz Pentium II, running Linux and being part of a MPI PC cluster. The software used was *M.DynaMix*.[32] Additionally, a CHARMM simulation was performed in vacuo at 300 K for 1 ns with the PARM22 force field.[33]

The atoms of the mannosyl group are designated with a prime. The torsional angles across the glycosidic linkage are defined as H1′−C1′−O3−C3 (ϕ) and H3−C3−O3−C1′ (ψ). For the investigation of the three-dimensional solvent structure around α-D-Man*p*-(1 → 3)-β-D-Glc*p*-OMe, the molecular reference coordinate system was fixed by the vectors O3−C1 and O3−C5′. For the calculation of the generalized order parameter (S^2) from the MD simulations the C2−C5 and C2−C3′ vectors were chosen for the reference system and the values of S^2 were obtained from the long time decay of the dipole−dipole autocorrelation function by extrapolating it to the ordinate (*y*-axis).

III. Results and Discussion

A. Water Solution. Conformations of a disaccharide molecule, such as α-D-Man*p*-(1 → 3)-β-D-Glc*p*-OMe (Figure 1), can be conveniently described in terms of the two torsional angles across the glycosidic linkage, namely ϕ and ψ. Vacuum simulations for both the GLYCAM and the OPLS models exhibit two main minima (potential wells) on the adiabatic energy surface close to g^- (−60°, well A) and g^+ (+60°, well B) conformations with respect to the ϕ torsional angle (Figure 2a). Although the values of the glycosidic torsional angles for both wells are very similar for GLYCAM and OPLS potential fields, their relative energies differ. The OPLS force field gives a preference for well A, which is about 5.0 kJ/mol more stable, compared to well B. The relative energies for the two wells, estimated using the GLYCAM parameter set, are very close to each other. Nevertheless, the A well is energetically (entropically) somewhat more favorable because of its wider confor-

(23) Jorgensen, W. L.; Chandrasekhar, J.; Madura, J. D.; Impey, R. W.; Klein, M. L. *J. Chem. Phys.* **1983**, *79*, 926−935.
(24) Berendsen, H. C. J.; Postma, J. P. M.; van Gunsteren, W. F.; Hermans, J. In *Intermolecular forces;* Pulman, B., Ed.; Reidel Publishing Co.: Dordrecht, The Netherlands, 1981; pp 333−342.
(25) Skaff, M. *J. Chem. Phys.* **1997**, *107*, 7996−8002.
(26) Luzar, A.; Chandler, D. *J. Chem. Phys.* **1993**, *98*, 8160−8173.
(27) Jorgensen, W. L., unpublished, see ref 25.
(28) van Gunsteren, W. F.; Berendsen, H. J. C. *Mol. Phys.* **1977**, *34*, 1311−1327.
(29) Nóse, N. *Mol. Phys.* **1984**, *52*, 255−268.
(30) Hoover, W. G. *Phys. Rev.* **1985**, *A31*, 1695−1697.
(31) Tuckerman, M.; Berne, B.J.; Martyna, G. J. *J. Chem. Phys.* **1992**, *97*, 1990−2001.
(32) Lyubartsev, A.; Laaksonen, A. *A scalable parallel general-purpose simulation software for arbitrary mixtures of molecules*, Stockholm University, 1998.
(33) Höög, C.; Widmalm, G., unpublished results.

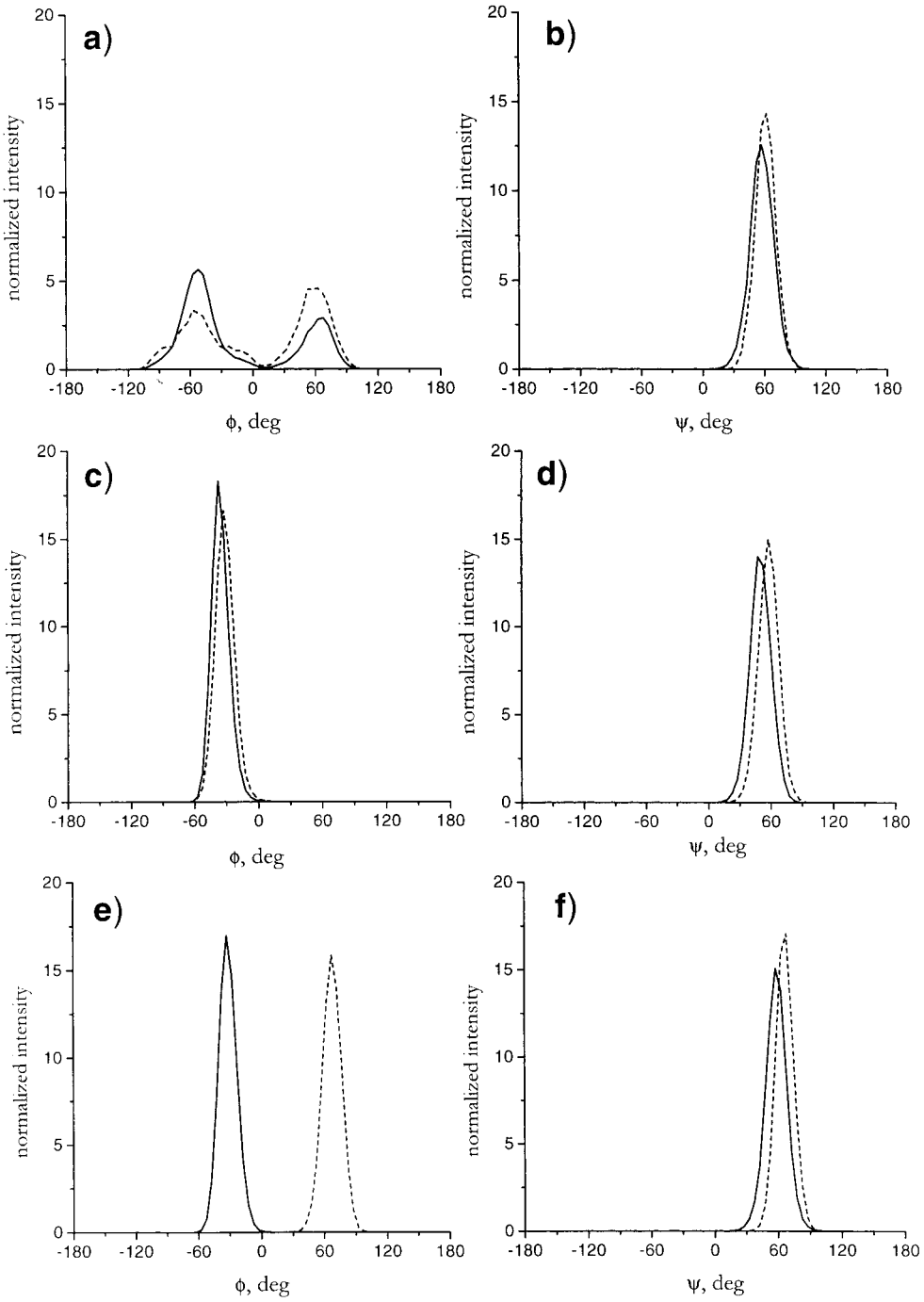

Figure 2. Distribution of the transglycosidic torsional angles H1′−C1′−O3−C3 (ϕ) and H3−C3−O3−C1′ (ψ) over trajectories. (a, b) Vacuum simulations V1 (- - -) and V2 (—). (c, d) Aqueous solutions W1 (- - -) and W3 (—). (e, f) Water−DMSO solutions M1 (- - -) and M2 (—).

mational space. Interestingly, for both force fields, the flexibility of the disaccharide is entirely connected to the behavior of the ϕ torsional angle. During the 1 ns simulations, the ψ torsional angle shows a very stable g^+ conformation (Figure 2b). This, in fact, occurs for all of the simulations in this work.

For a comparison, a 1.0 ns MD simulation was performed using the CHARMM/PARM22 force field in vacuo. The results were similar to those obtained from the simulations in aqueous solutions using the GLYCAM and OPLS force fields, giving the A well as the major state, with the angle $\phi = -37°$ (rmsd 9°) over an 800 ps trajectory. One single transition of the ϕ torsional angle to the B well occurs after about 900 ps, where the molecule stays for about 40 ps before returning back to well A. The ψ torsional angle shows no large conformational changes. However, the angle $\psi = 38°$ (rmsd 18°) over an 800 ps trajectory, showed significantly larger fluctuations than ϕ.

Conformation A is stabilized by an intramolecular hydrogen bond between hydroxyl groups of O6′ and O2 in the different sugar residues. It is not expected that carbohydrates in aqueous solutions are found in their vacuum energy-minimized conformations. This is because water molecules from the solvent readily form hydrogen bonds between the hydroxyl groups, which can serve both as hydrogen bond donors and acceptors. For example, a conformational transition of α-D-Man*p*-(1 → 3)-*β*-D-Glc*p*-OMe from well A to well B, while breaking the inter-residue hydrogen bond, is likely to be accompanied by formation of new hydrogen bonds to the solvent and new water bridges between different sugar oxygens. Indeed, three main

Table 3. Trajectory-Averaged Values of Torsional Angles across the Glycosidic Linkage and Their Root Mean Square Deviations

trajectory	ϕ (deg)	$\Delta\phi$ (deg)	ψ (deg)	$\Delta\psi$ (deg)
GLYCAM, vacuum, well A	−56.5	22.2	58.6	16.4
GLYCAM, vacuum, well B	58.3	21.1	61.2	18.3
OPLS, vacuum, well A	−56.3	20.0	58.5	16.4
OPLS, vacuum, well B	62.3	27.1	58.9	17.0
GLYCAM−SPC	−31.5	12.6	57.5	12.8
OPLS−TIP3P	−35.4	14.8	49.9	19.7
GLYCAM−SPC−P2	67.2	12.6	62.1	16.5
GLYCAM−TIP3P−OPLS	−31.6	12.7	58.1	19.2

contributions to the transition free energy can be identified: (i) intramolecular terms, (ii) change in ethalpy of the solvent−solute interactions, and (iii) change in entropy of the solvent. The entropy contribution is difficult to measure, both experimentally and in computer simulations. In the latter case it depends significantly on the choice of the force field for solute and solvent molecules.

Experimental estimation of the H1′−H3 interatomic distance for α-D-Man*p*-(1 → 3)-β-D-Glc*p*-OMe in water−DMSO solution at 288 K gives a value of 2.45 Å.[5] From the simulations we obtain for the A well a distance of 2.35 Å with GLYCAM and 2.34 Å with the OPLS force field. These values can be compared to the value of approximately 3.3 Å for the B well, obtained for both force fields. This strongly supports the fact that the A conformer is preferred in water solution. Our MD simulations of α-D-Man*p*-(1 → 3)-β-D-Glc*p*-OMe in water show a clear preference for the A conformation, which is evident from the distribution over the glycosidic torsional angles (see Figure 2c,d). Observe, however, that the maxima of the distributions in aqueous solutions are considerably shifted, compared to those obtained from the vacuum simulations.

It should be mentioned that we did try both of the wells A and B as initial conformations in our MD simulations. The simulations in water, started from the B well, underwent a rapid transition to the A well. In all three disaccharide−water simulations, the A well was found to be the most stable conformation with a shift of about 15° for the ϕ torsional angle (Figure 2c,d) compared to the vacuum simulations. The average values of the main torsional angles together with their root-mean-square (rms) deviations are given in Table 3. Although a rapid rotation of the glucose methoxy group was observed in vacuum simulations around the β-glycosidic linkage, the distribution of the Hl−Cl−Ol−C_{methyl} torsional angles in water solution showed a very strong preference for g^+ conformations.

During all of the simulations both the mannose and glucose rings stayed in the $^4C_1$ conformation, correctly representing the anticipated behavior. A detailed analysis of the molecular geometry trajectories for the GLYCAM and OPLS force fields, however, showed certain differences between the two models. Simulations with the GLYCAM force field showed almost ideal pyranoid rings with all endo-cyclic torsional angles, being close to *gauche* conformations. In the simulations using the OPLS force field, the torsions for the endo-cyclic COCC turned out to be considerably shifted (up to 15°) from ideal *gauche* conformations. The hydroxymethyl group in the glucosyl residue exhibited all three staggered conformations, giving a preference for the g^+ conformer for both force fields, with a rapidly rotating hydroxyl group. Significant differences were found in the conformational behavior of the secondary hydroxyl groups. In contrast to our vacuum simulations and the results of Brady and coworkers[10] for trehalose with a CHARMM force field, most hydroxyl groups of α-D-Man*p*-(1 → 3)-β-D-Glc*p*-OMe exhibited stable conformations using the GLYCAM force field. At least, no rapid rotation of the secondary hydroxyl groups was observed. For the OPLS parameter set of Damm et al.,[16] the conformational behavior of the secondary hydroxyl groups, showed fast oscillations between distorted g^+ and g^- conformations with respect to the HCOH angle. The rather different conformational behavior of the hydroxyl groups using OPLS caused a corresponding difference in the geometry of the O6′−O2 intramolecular hydrogen bond. This was found to be fairly stable in all the three simulations in aqueous solution, persisting 78, 77, and 60% of the time in W1, W2, and W3 trajectories, respectively.

In the simulations with the GLYCAM force field, the hydroxyl group attached to the C2 atom of the glucosyl residue serves as a donor of an intramolecular hydrogen bond, while it was generally found to be an acceptor when the OPLS force field was used. Moreover, in the W3 system both the O6′−O2 and O2−O5′ hydrogen bonds were present, and the geometry of both pairs satisfied our hydrogen bond criteria over 10% of the trajectory time.

Differences in the molecular geometry can easily affect the hydration around the disaccharide molecule. The number of hydrogen bonds between the disaccharide molecule and the solvent molecules could be used to establish a more complete picture of hydration around α-D-Man*p*-(1 → 3)-β-D-Glc*p*-OMe. For the purpose of identifying the hydrogen bonds we have used the following geometric criteria, considering a hydrogen bond as an interaction having an oxygen−oxygen distance less than 3.4 Å and the donor−proton−acceptor angle larger than 120°. The averaged numbers of hydrogen bonds for each sugar oxygen from the three aqueous solutions are given in Table 4. Except for the O6′ and O2 groups, the total average number of hydrogen bonds for the solute oxygens is of same order of magnitude in all three simulations, but varies substantially from oxygen to oxygen. This behavior is opposite to what was previously observed for maltose[9] and trehalose,[10] simulated using a CHARMM force field. The intramolecular hydrogen bond between the O6′ and O2 groups reduces their ability to bond to the solvent and shields the O5′ atom, which on average forms fewer bonds with water, compared to the corresponding atoms of trehalose.[10] The other hydroxyl groups form on average somewhat fewer hydrogen bonds than those observed in maltose and trehalose simulations.[9,10] The only exception is the O6 atom in the glucosyl residue, which is the most accessible hydroxyl group of the α-D-Man*p*-(1 → 3)-β-D-Glc*p*-OMe molecule. It is also capable of rotating fairly rapidly.

In aqueous solution, the geometry of α-D-Man*p*-(1 → 3)-β-D-Glc*p*-OMe does not favor inter-residue hydrogen-bond bridging, except for the O6′ and O2 atoms. These two atoms share the same water molecule through more than 50% of the 1.0 ns simulation. In GLYCAM−SPC and GLYCAM−TIP3P simulations, a noticeable bridging via a water molecule was observed between O2′ and O3′, O3′ and O4′, O1 and O5 as well as the O2 and O1 atoms, although in all cases it was less than 10% of the duration of the whole simulations.

The large number of hydrophilic centers in carbohydrates imposes a strong anisotropic structuring on the surrounding solvent. This structuring can be demonstrated by a three-dimensional local density profile, calculated from the surrounding solvent molecules, in a reference coordinate system attached to the disaccharide molecule. We have used the O3−C1 and O3−C5′ vectors to fix the reference coordinate frame. Figure 3 shows the time-averaged positions for each sugar atom in this reference coordinate frame and contours of large positive

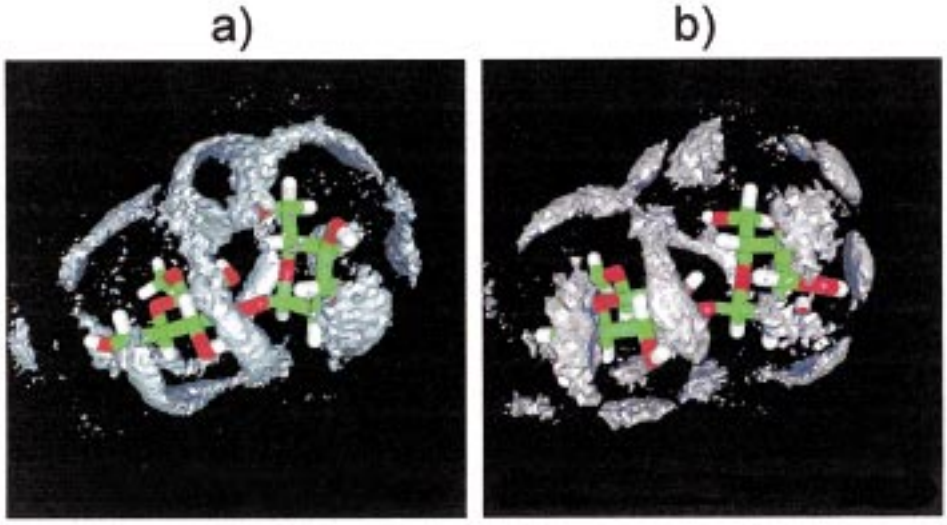

Figure 3. Spatial distribution functions of water oxygens around α-D-Man*p*-(1 → 3)-*β*-D-Glc*p*-OMe. Contours show the regions of high positive deviations of the local density (3 times higher than the average value). (a) System W1, (b) system W3.

Table 4. Trajectory-Averaged Number of Hydrogen Bonds to Water Made by Each Oxygen Atom of α-D-Man*p*-(1 → 3)-*β*-D-Glc*p*-OMe

oxygen atom	trajectory	number of hydrogen bonds		
		donated	accepted	total
O5′	W1		0.14	0.14
	W2		0.15	0.15
	W3		0.14	0.14
O2′	W1	0.53	1.13	1.66
	W2	0.55	1.05	1.60
	W3	0.78	1.24	2.02
O3′	W1	0.41	1.18	1.59
	W2	0.60	1.31	1.19
	W3	0.49	1.53	2.02
O4′	W1	0.57	1.68	2.25
	W2	0.72	1.70	2.42
	W3	0.58	1.24	1.82
O6′	W1	0.12	1.60	1.72
	W2	0.11	1.60	1.71
	W3	0.60	1.25	1.85
O5	W1		0.83	0.83
	W2		0.84	0.84
	W3		0.61	0.61
O2	W1	0.62	0.95	1.57
	W2	0.68	0.87	1.55
	W3	0.21	1.25	1.46
O3	W1		0.01	0.01
	W2		0.02	0.02
	W3		0.06	0.06
O4	W1	0.80	1.46	2.26
	W2	0.86	1.53	2.39
	W3	0.89	1.33	2.22
O6	W1	0.86	1.66	2.52
	W2	0.86	1.68	2.54
	W3	0.88	1.57	2.45
O1	W1		0.82	0.82
	W2		0.82	0.82
	W3		1.11	1.11
in total	W1			15.4
	W2			15.9
	W3			15.8

deviations of the local oxygen density from its average bulk value in simulations W1 and W3, respectively. The isodensity surfaces of the water oxygens in Figure 3 are chosen as 3 times the value of oxygen density in bulk water. Water molecules around the disaccharide molecule form at least two pronounced solvation shells. The largest intensities are observed near the hydroxyl groups of the disaccharide. Distinct band-shaped clouds are formed by the water molecules serving as hydrogen bond donors around sugar oxygens. The water molecules, acting as hydrogen bond acceptors, form more spherical clouds near hydroxyl protons of the solute. The water structuring was found to be similar in systems W1 and W2, where different models for water were used with the GLYCAM force field. Thus, no substantial model dependence was observed in the solvation structure for water. While three-dimensional density profiles for the different force fields (GLYCAM and OPLS) also exhibit similar main features, there are some marked differences in the anisotropic structuring. These differences are most likely due to different orientations of hydroxyl groups with respect to the disaccharide per se. The variation in orientation is especially pronounced around the O6′ and O2 atoms.

It is worth mentioning that in spite of the lower number of hydrogen bonds formed by α-D-Man*p*-(1 → 3)-*β*-D-Glc*p*-OMe compared to the simulations of trehalose,[10] the water structuring around the disaccharide molecule is as strong as that observed by Brady and coworkers.[10] Internal motions tend to smear out the clouds of high solvent density, and the choice of the reference coordinate system may partly explain the observed differences. The rms fluctuations of the glycosidic torsional angles in trehalose were approximately 13° for the structure suggested to be the global minimum free-energy conformation in solution. The flexibility of α-D-Man*p*-(1 → 3)-*β*-D-Glc*p*-OMe in a conformational well is quite similar for ϕ in solution, and only slightly larger for ψ (Table 2).

At this stage, we compare the conformations of α-D-Man*p*-(1 → 3)-*β*-D-Glc*p*-OMe to similar disaccharides previously studied, i.e., α-D-Man*p*-(1 → 3)-α-D-Man*p*-OMe,[34] and α-D-Glc*p*-(1 → 3)-D-Glc*p*,[35] where the configuration at C2 and C2′, respectively, are changed compared to the disaccharide in the present simulation. Molecular modeling of carbohydrates in vacuo may lead to low-energy conformers stabilized by hydrogen bonding, which are not significantly populated when modeled in solution or as determined by experimental data, e.g., NMR spectroscopy.[36] However, results from simulation of

(34) Imberty, A.; Tran, V.; Prez, S. *J. Comput. Chem.* **1989**, *11*, 205−216.

(35) Dowd, M. K.; Zeng, J.; French, A. D.; Reilly, P. J. *Carbohydr. Res.* **1992**, *230*, 223−244.

(36) Kroon-Batenburg, L. M. J.; Kroon, J. *Biopolymers* **1990**, *29*, 1243−1248.

oligosaccharide conformation in vacuo and in solution may also be quite similar.[37]

The present simulations of 1 ns in vacuo showed two conformational states for the ϕ torsional angle, using either force field. When the disaccharide was simulated in water, one conformational state was observed. This conformation is stabilized by the exo-anomeric effect.[38] In conformational analysis of disaccharides, a Ramachandran map can reveal one low-energy state at the global energy minimum[39] or two states of low-energy, bimodal for the ψ torsional angle, one of which is the global energy minimum.[14] However, the barrier to interconversion between these states may be low, on the order of kT or less,[40] in which case the sampling of the conformational region is rapid.

Conformational analysis of α-D-Man*p*-(1 → 3)-α-D-Man*p*-OMe[34] and α-D-Glc*p*-(1 → 3)-D-Glc*p*[35] based on Ramachandran maps reveals a bimodal shape along the ψ torsional angle for both disaccharides. In α-D-Man*p*-(1 → 3)-α-D-Man*p*-OMe a hydrogen bond HO6′ to O2 is identified, similar to that found in the present simulation. A low-energy region corresponding to well B in our simulation is readily identified for α-D-Man*p*-(1 → 3)-α-D-Man*p*-OMe. Furthermore, when the hydroxymethyl groups have the g^+ conformation, the energy difference between the conformational states corresponding to wells A and B is only 5.4 kJ/mol for the energy-minimized molecules. Thus, the B well for α-D-Man*p*-(1 → 3)-α-D-Man*p*-OMe is energetically accessible, also when modeled using MM3.[41] For α-D-Glc*p*-(1 → 3)-D-Glc*p* a plateau region occurs where the B well exists. In β-nigerose (α-D-Glc*p*-(1 → 3)-β-D-Glc*p*) a local energy minimum could be identified about 21 kJ/mol above the global energy minimum (well A). For α-nigerose (α-D-Glc*p*-(1 → 3)-α-D-Glc*p*) only a plateau region was observed. Thus, the region corresponding to well B is not significantly populated in nigerose, i.e., when the terminal sugar residue is glucose (which has an equatorial hydroxyl group at C2′).

If the simulations of α-D-Man*p*-(1 → 3)-β-D-Glc*p*-OMe in water were extended, it is probable that well B would be populated to some degree. The present simulations did not show a bimodal occurrence for the ψ torsional angle. The above reasoning is in agreement with the CHARMM simulation which shows an "extended A well" with flexibility along the ψ torsional angle as well as a transition to and from well B. It can be anticipated that the increased flexibility along the ϕ torsional angle of the α-linked mannosyl residue can be related to the configuration of the axial hydroxyl group at C2′.

B. Water/DMSO Solution. The solvent structure of water around α-D-Man*p*-(1 → 3)-β-D-Glc*p*-OMe is complex and the conformational behavior of the solute is strongly affected by hydration. In this section we consider the solvation of α-D-Man*p*-(1 → 3)-β-D-Glc*p*-OMe in the binary 1:3 molar mixture of DMSO and water. This composition is often used in experimental studies of complex organic molecules due to its higher viscosity and exceptionally low freezing temperature, which both are helpful in NMR studies of the internal motion of the solute.

Two different sets of solvent models (see Section II) were used for the simulation of the α-D-Man*p*-(1 → 3)-β-D-Glc*p*-OMe−water/DMSO solution, while the force field for the solute was the same. Again, both the A and B wells were initially tested as starting conformations. This time α-D-Man*p*-(1 → 3)-β-D-Glc*p*-OMe was found to be stabilized as different conformers in the two solvent models of water/DMSO. The simulation with TIP3P−OPLS solvent potentials (system M2) preferred the A conformer, while conformer B was found to be stable in the simulation where the SPC−P2 set of potentials (system M1) was used for water/DMSO. The torsional angles ϕ and ψ (Figure 2e,f) are slightly shifted from the corresponding vacuum values (Figure 2a,b).

Table 5. Trajectory-Averaged Number of Hydrogen Bonds to Water and Dimethylsulfoxide Made by Each Oxygen Atom of α-D-Man*p*-(1 → 3)-β-D-Glc*p*-OMe

		number of hydrogen bonds			
oxygen atom	model of the solvent	donated water	accepted water	donated DMSO	in total
O5′	M1		0.09		0.09
	M2		0.19		0.19
O2′	M1	0.49	0.37	0.13	0.99
	M2	0.50	0.99	0.04	1.53
O3′	M1	0.39	1.01	0.22	1.62
	M2	0.60	1.05	0.09	1.74
O4′	M1	0.38	1.02	0.24	1.64
	M2	0.42	1.46	0.19	2.07
O6′	M1	0.13	1.13	0.65	1.91
	M2	0.11	1.14	0.04	1.29
O5	M1		0.63		0.63
	M2		0.27		0.27
O2	M1	0.10	0.09	0.71	0.90
	M2	0.23	0.82	0.41	1.46
O3	M1		0.02		0.02
	M2		0.02		0.02
O4	M1	0.52	1.08	0.24	1.84
	M2	0.41	1.37	0.47	2.25
O6	M1	0.81	1.48	0.14	2.43
	M2	0.54	1.18	0.30	2.02
O1	M1		0.63		0.63
	M2		0.20		0.20
in total	M1	2.82	7.55	2.33	12.7
	M2	2.81	8.69	1.54	13.0

The preference for the A conformer agrees with experimental NMR measurements.[5] However, we investigated the solvation around both conformers and, correspondingly, both solvent models. Due to the lower number of molecules of both types in the solvent mixture (compared for example to the simulations with pure water as solvent), it is difficult to draw any conclusions concerning the properties of the two mixed solvent models as bulk liquids. Nevertheless, the M1 simulation gave a significantly larger average density (1.075 g/cm^3), compared to the M2 run (1.052 g/cm^3). Such a difference is difficult to explain based only on the larger effective diameters of sulfur and CH_3 sites of the DMSO molecule in the OPLS model. Another significant factor should be the number of hydrogen bonds between the different components in the solvent, which was found to be larger for the SPC−P2 model.

In general, addition of DMSO into the water solution leads to a decrease in the total number of solute−solvent hydrogen bonds. To some extent, water and DMSO molecules compete with each other as prospective acceptors of the hydrogen bonds donated by the hydroxyl groups of α-D-Man*p*-(1 → 3)-β-D-Glc*p*-OMe. Only water molecules can serve as hydrogen bond donors to the solute. This gives water a clear advantage in entering the first solvation shell. This preference for water is more pronounced in the GLYCAM−TIP3P−OPLS system (Table 5). Obviously, when more water is present in the first shell, the number of hydrogen bonds between the disaccharide and DMSO

(37) Hardy, B. J.; Egan, W.; Widmalm, G. *Int. J. Biol. Macromol.* **1995**, *17*, 149−160.
(38) Tvaroska, I.; Carver, J. P. *J. Phys. Chem.* **1995**, *99*, 6234−6241.
(39) Jansson, P.-E.; Kenne, L.; Persson, K.; Widmalm, G. *J. Chem. Soc., Perkin Trans. 1* **1990**, 591−598.
(40) Odelius, M.; Laaksonen, A.; Widmalm, G. *J. Phys. Chem.* **1995**, *99*, 12686−12692.
(41) Dowd, M. K.; French, A. D.; Reilly, P. J. *J. Carbohydr. Chem.* **1995**, *14*, 589−600.

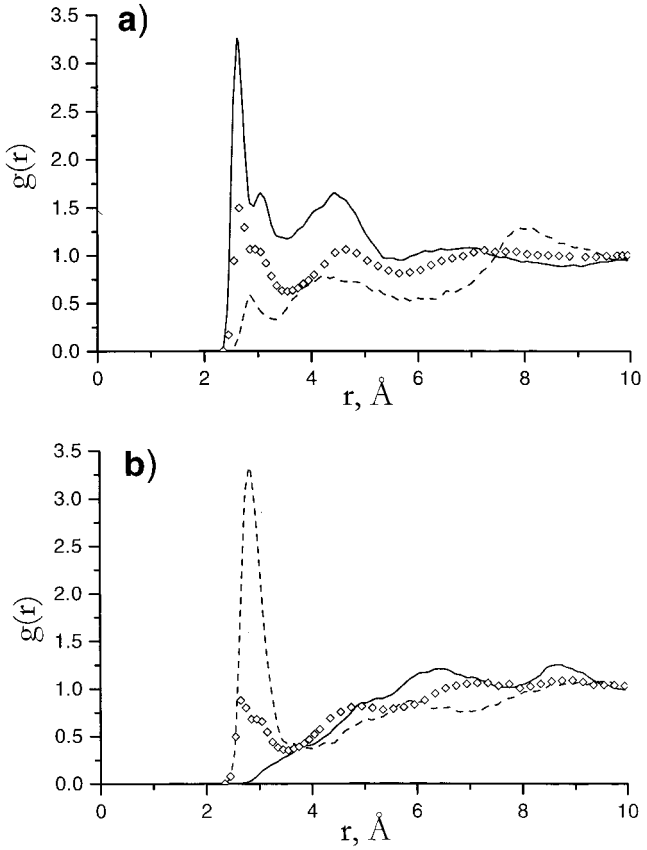

Figure 4. O−O radial distribution functions for two different disaccharide oxygens (a) O2 and (b) O6′ in water−DMSO solution (system Ml): $O_{sugar}-O_{H_2O}$ (—), $O_{sugar}-O_{DMSO}$ (- - -). Squares show $O_{sugar}-O_{H_2O}$ radial distribution functions for the corresponding aqueous solution (run W1).

molecules is reduced. The number of hydrogen bonds to DMSO appears to be considerably higher in the simulation of the M1 system.

In comparing the average total number of solute−solvent hydrogen bonds, we should take into account that the A conformer of α-D-Man*p*-(1 → 3)-*β*-D-Glc*p*-OMe is less exposed to the solvent molecules than the B conformer, observed in the SPC−P2 solvent mixture (system M1). This is due to the O6′−O2 hydrogen bond, observed in the TIP3P−OPLS solution (system M2—as well as in all the simulated aqueous solutions), is broken in the B conformer. Despite this, the total number of hydrogen bonds was found to be larger for the TIP3P−OPLS solvent, where most of these bonds to the solute were formed by the water molecules.

It is worth noting, that the different hydroxyl groups of the disaccharide are *selectively* solvated by the two components of the solvent as hydrogen bond acceptors (Table 5). Figure 4 shows the $O_{sugar}-O_{water}$ radial distribution functions (RDF) for the two different oxygen atoms O2 and O6′ of α-D-Man*p*-(1 → 3)-*β*-D-Glc*p*-OMe for the M1 system together with those from the corresponding aqueous solution (W1). For pure water as a solvent, the first peaks of the RDFs are fairly pronounced. When DMSO is added, the first peak grows much higher for the O6′ atom, while it is lacking for O2. At the same time a very high peak arises between the water oxygens and O2. These preferences for different oxygen atoms of the disaccharide to attract either water or DMSO can be seen in Figure 5, showing regions of excess partial local densities for both components from their bulk values. Oxygens of DMSO form drop-shaped clouds near the hydroxyl protons of the disaccharide, while water molecules form banana-shaped clouds around oxygen atoms, creating hydrogen bonds to α-D-Man*p*-(1 → 3)-*β*-D-Glc*p*-OMe by donating their own protons. It is particularly interesting to observe that the O2 atom, serving as the intramolecular hydrogen bond acceptor in the A conformation, gives a certain preference for DMSO as a hydrogen bond acceptor (see Table 5 and Figure 5b). In conformation B, where the intramolecular hydrogen bond between O6′ and O2 is broken, both oxygen atoms show a clear preference for DMSO.

The reasons for the behavior of different hydroxyl groups in the mixed solvent need to be investigated further. However, estimation of the residence time for different oxygens of the disaccharide and water, using criteria taken from the work by Lyubartsev and Laaksonen,[42] gives values from 10 to 45 ps; residence times for $O2-O_{DMSO}$ pairs are equal to 36.2 and 14.0 ps for SPC−P2 and TIP3P−OPLS models, respectively. These are typical values for a hydrogen bond residence time (and much smaller compared to the total length of the simulation).

The reorientational time correlation functions $\langle P_2(\vec{\mu}(0)\cdot\vec{\mu}(t))\rangle$ are shown in Figure 6 for the overall motion of α-D-Man*p*-(1 → 3)-*β*-D-Glc*p*-OMe in the water solutions W1 and W3 and in the water−DMSO mixture M1. μ is a unit vector coinciding with the dipole moment of disaccharide. For the GLYCAM−SPC (W1) and OPLS−TIP3P (W3), corresponding correlation times are estimated to 130 ps and 90 ps, respectively. For the GLYCAM−TIP3P system (not shown in the figure), the correlation time is 70 ps. Obviously, the reorientational motion of α-D-Man*p*-(1 → 3)-*β*-D-Glc*p*-OMe is very much dependent on the water model used in the simulation. The flexible SPC model is apparently a more viscous medium than the the rigid TIP3P. The corresponding reorientational correlation times for α-D-Man*p*-(1 → 3)-*β*-D-Glc*p*-OMe in the mixed solvent are much longer. These are 700 ps for the GLYCAM−SPC−P2 system and 500 ps for GLYCAM−TIP3P−OPLS. The experimental[5] value is 800 ps in the mixed solvent.

C. Comparison with NMR Results. MD simulations, covering nanosecond time-scales, allow a direct comparison of a number of parameters characterizing both conformation and dynamics of disaccharides with those obtained experimentally. In this section we compare our simulation results with the experimental findings of the NMR study by Mäler et al.,[5] where the variable field and the variable temperature carbon-13 relaxation data for α-D-Man*p*-(1 → 3)-*β*-D-Glc*p*-OMe were interpreted in terms of the Lipari−Szabo model.[43] The dynamical parameters thus obtained were used, together with the proton cross-relaxation rates for the proton pairs H1′−H2′ and H1′−H3, to obtain the two proton−proton distances. In Table 6, we report some simulated data related to the experimental results. The central quantity of the Lipari−Szabo model is the generalized order parameter S^2 given as

$$S^2 = \frac{4\pi}{5}\sum_{m=-2}^{2} |\langle Y_{2m}(\Omega)\rangle|^2 \qquad (1)$$

$Y_{2m}(\Omega)$ is the rank two spherical harmonics, and Ω is the polar angle of the selected axis with the respect to a reference frame rigidly attached to the molecule. In our case, the selected axes are the internuclear H1′−H2′ and H1′−H3 axes, i.e., the principal axes of the corresponding dipole−dipole interactions, while the reference frame is attached to the C2′−C5′ and C2′−C3 vectors.

(42) Lyubartsev, A.; Laaksonen, A. *J. Phys. Chem.* **1996**, *100*, 16410−16418.

(43) Lipari, G.; Szabo, A. *J. Am. Chem. Soc.* **1982**, *104*, 4546−4555.

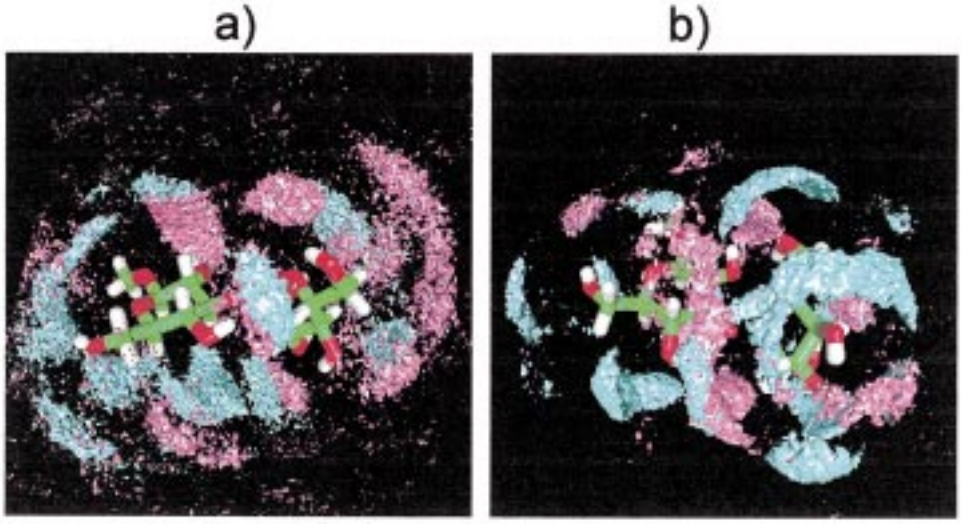

Figure 5. Spatial distribution functions of water (in blue) and DMSO oxygens (in red) around the α-D-Man*p*-(1 → 3)-β-D-Glc*p*-OMe molecule. Contours show the regions of high positive deviations of the local density (4 times higher than the average value). (a) System M1. (b) System M2.

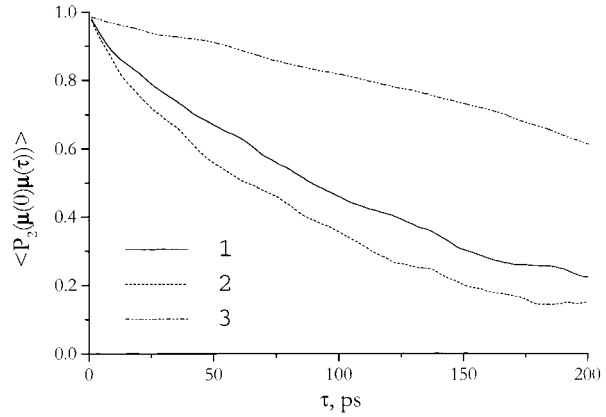

Figure 6. Reorientational time correlation functions for the rank 2 spherical harmonics, calculated in coordinates fixed in the disaccharide. Systems W1 (1), W3 (2), and M1 (3).

Table 6. Interatomic Distances and Order Parameters for H1′−H2′ and H1′−H3 Proton Pairs

	H1′−H2′				H1′−H3			
trajectory	r, Å	$\langle r^{-3}\rangle^{-1/3}$	S^2	S^{2*}	r, Å	$\langle r^{-3}\rangle^{-1/3}$	S^2	S^{2*}
W1	2.50	2.49	0.986	0.969	2.35	2.33	0.963	0.961
W2	2.49	2.49	0.985	0.967	2.36	2.34	0.970	0.935
M1	2.53	2.53	0.989	0.976	3.28	3.27	0.985	0.957
M2	2.50	2.49	0.984	0.964	2.35	2.33	0.982	0.959
exp, water−DMSO	2.63				2.45			

The S^2 in eq 1 is identical to the angular order parameter, as defined by Brüschweiler et al.[44] These authors introduce another order parameter taking into consideration not only the fluctuations of Ω (angular fluctuations), but also those of internuclear distance (radial fluctuations). We denote this quantity S^{2*}.

$$S_{ij}^{2*} = \frac{4\pi}{5}\left\langle\frac{1}{r_{ij}^6}\right\rangle^{-1}\sum_{m=-2}^{2}\left|\left\langle\frac{Y_{2m}(\Omega)}{r_{ij}^3}\right\rangle\right|^2 \qquad (2)$$

The subscript *ij* refers to a pair of nuclei. By means of MD simulations, Brüschweiler et al.[44] also demonstrated that S_{ij}^{2*} could, to a good approximation, be expressed as a product of S^2 and the radial factor $\langle r_{ij}^3\rangle^2/\langle r_{ij}^6\rangle$. The quantities S^2 and S^{2*}, from the present simulation, are compared to each other in Table 6. The values of S^2 are calculated as the long-time plateaus of the appropriate time-correlation functions (in the local coordinate systems) from MD simulations. Table 6 also contains the mean values of r_{ij} and of $\langle r_{ij}^{-3}\rangle^{-1/3}$. The latter quantity is directly related to the dipolar coupling constant, the interaction strength of an important interaction studied by NMR spectroscopy.

We note that the order parameters from the simulations are in all cases close to unity, which is consistent with the picture of a fairly rigid molecule. This picture is further confirmed by the agreement between the two types of mean distances. The experimental order parameters from the work of Mäler et al. are lower. There are two possible interpretations of this difference: either the force field makes the molecule too rigid, or the experimental order parameters are underestimated. In fact, we lean towards the second interpretation. In the analysis of the carbon-13 relaxation experiments, which formed the base of the estimation of S^2, Mäler et al. assumed a carbon−proton distance of 1.098 Å, corresponding to the carbon−proton coupling constant (DCC) of 22.82 kHz. This DCC may actually be an overestimation. Nakai et al.[45] determined the DCC for a directly bonded carbon−proton pair in calcium formate by solid-state NMR and reported the appropriately vibrationally averaged "effective" CH distance of 1.13 Å. If this value had been applied in the study by Mäler et al.,[5] a higher value of the order parameter would have been obtained.

A comparison of the results of different simulations in Table 6 leads to conclusions in agreement with the conformational analysis above. While all of the simulations agree on the estimates of the mean H1′−H2′ distance, the M1 simulation gives a strongly deviating inter-residue distance H1′−H3.

IV. Conclusions

The present work attempts to establish several important structural and dynamical features of α-D-Man*p*-(1 → 3)-β-D-Glc*p*-OMe in pure water and water−DMSO mixed solutions through a series of a nanosecond molecular dynamics simulations. The results can be directly compared with the experimental observations of Mäler et al.[5] The simulations were carried out

(44) Brüschweiler, R.; Roux, B.; Blackledge, M.; Giesinger, C.; Karplus, M.; Ernst, R. R. *J. Am. Chem. Soc.* **1992**, *114*, 2289−2302.

(45) Nakai, T.; Ashida, J.; Terao, T. *Mol. Phys.* **1989**, *67*, 839−847.

using two different force fields for α-D-Man*p*-(1 → 3)-*β*-D-Glc*p*-OMe: GLYCAM and OPLS models, both recently developed. In addition, different potential functions were employed for the solvent components available to us to compare our models with the experimental data.

The vacuum simulations with the GLYCAM and OPLS models showed two main minima (wells A and B) on the adiabatic energy map (see Figure 2a,b). However, in water solution the disaccharide showed a clear preference for well A, irrespective of the model used. This is also in agreement with the previous experimental findings.[5] The hydroxyl groups were found to be extensively hydrogen-bonded to surrounding water molecules; the average number of hydrogen bonds, made by the hydroxyl groups of the solute and the main features of the anisotropic water structuring around the disaccharide, were found to be quite similar for different potential models used both for α-D-Man*p*-(1 → 3)-*β*-D-Glc*p*-OMe and water.

In one of the two simulated mixed water−DMSO solutions, using the GLYCAM force field (GLYCAM−SPC−P2 system), α-D-Man*p*-(1 → 3)-*β*-D-Glc*p*-OMe showed a preference for the B well. This is, however, not in agreement with experimental observations. In general, adding DMSO to an aqueous solution leads to a decrease of the total number of hydrogen bonds formed between α-D-Man*p*-(1 → 3)-*β*-D-Glc*p*-OMe and solvent sites. Also, different hydroxyl groups of the disaccharide revealed a preference for different components of the solvent as hydrogen bond acceptors. Consequently, the anisotropic solvent structuring is quite complex in this case: areas with a relatively high partial local density for either water or DMSO can be distinguished in the first solvation shell. However, when we changed the solvent potential model, (GLYCAM−TIP3P−OPLS system), the A conformation was found to be stable. Similar to results in the GLYCAM−SPC−P2 system, different hydroxyl groups of the disaccharide preferred different components of the solvent as hydrogen bond acceptors.

The observed solvent model dependence of the behavior of the disaccharide is, of course, discouraging. It clearly shows that potential models have to be chosen with care and that reliable experimental data are needed for evaluation of force fields. Especially for complex solvents with a large number of competing interactions, the proper balance between them is easily shifted. The reasons for such model dependence in the disaccharide conformation and anisotropic structuring of the solvent imposed by the disaccharide need to be investigated further.

As was suggested, the hydration is probably dominated by the first-shell structuring in the solvent.[22,46] The optimal hydration might be achieved, when both the solute and the solvent have a topology, which allows the best compatibility for the hydration requirements of adjacent functional groups. This further highlights the dependence of the complex solvent structuring and the conformational behavior of the disaccharide on the potential model used for the solvent, especially in the case when different models produce different representations of the internal structure of the solute.

Acknowledgment. This work has been supported by the Swedish Natural Science Research Council (NFR), the Nordic Minister Council and the Swedish Institute (A.V.).

JA9835180

(46) Galema, S. A.; Howard, E.; Engberts, J. B. F. N.; Grigera, J. R. *Carbohydr. Res.* **1994**, *265*, 215−225.